ARTICLE
Journal of Cellular Biochemistry 106:444–452 (2009)

Journal of Cellular Biochemistry

Protein Kinase-A Affects Sorting and Conformation of the Sodium-Dependent Glucose Co-Transporter SGLT1

Supriya Subramanian,[1] Petra Glitz,[1] Helmut Kipp,[2] Rolf K.H. Kinne,[1] and Francisco Castaneda[1*]

[1]*Max Planck Institute of Molecular Physiology, Otto-Hahn Straße 11, 44227 Dortmund, Germany*

[2]*Institute of Anatomy, University of Würzburg, D-97070 Würzburg, Germany*

ABSTRACT

In Chinese hamster ovary cells expressing rabbit sodium-dependent glucose transporter (rbSGLT1) protein kinase A (PKA) activators (forskolin and 8-Br-cAMP) stimulated α-methyl D-glucopyranoside uptake. Kinetic analysis revealed an increase in both V_{max} and affinity of the transport. Immunohistochemistry and biotinylation experiments showed that this stimulation was accompanied by an increased amount of SGLT1 localized into the plasma membrane, which explains the higher V_{max} of the transport. Cytochalasin D only partly attenuated the effect of forskolin as did deletion of the PKA phosphorylation site of SGLT1 in transient transfection studies. Experiments using an anti-phosphopeptide antibody revealed that forskolin also increased the extent of phosphorylation of SGLT1 in the membrane fraction. These results suggested that regulation of SGLT1 mediated glucose transport involves an additional direct effect on SGLT1 by phosphorylation. To evaluate this assumption further, phosphorylation studies of recombinant human SGLT1 (hSGLT1) in vitro were performed. In the presence of the catalytic subunit PKA and [^{32}P] ATP 1.05 mol of phosphate were incorporated/mol of hSGLT1. Additionally, phosphorylated hSGLT1 demonstrated a reduction in tryptophan fluorescence intensity and a higher quenching by the hydrophilic Trp quencher acrylamide, particularly in the presence of D-glucose. These results indicate that PKA-mediated phosphorylation of SGLT1 changes the conformation of the empty carrier and the glucose carrier complex, probably causing the increase in transport affinity. Thus, PKA-mediated phosphorylation of the transporter represents a further mechanism in the regulation of SGLT1-mediated glucose transport in epithelial cells, in addition to a change in surface membrane expression. J. Cell. Biochem. 106: 444–452, 2009.

KEY WORDS: ACTIVE TRANSPORT; α-METHYL-D-GLUCOPYRANOSIDE; KINETIC STUDIES; PROTEIN KINASE-A; SGLT1; STERN-VOLMER QUENCHING CONSTANT

The sodium/D-glucose co-transporter SGLT1 is a high affinity glucose transporter that utilizes the electrochemical gradient of sodium to drive the transport of sugar across the intestinal and renal brush border membranes with a sodium to glucose coupling ratio of 2:1. The regulation of the activity of SGLT1 has been studied using different in vitro systems (oocytes, brush border membranes, enterocytes) and in vivo systems (rat jejunum). Studies on oocytes expressing rabbit SGLT1 (rbSGLT) [Wright et al., 1996, 1997] have demonstrated the participation of protein kinase A (PKA) and protein kinase C in the regulation of SGLT1 mediated sugar transport. Stimulation of PKA leads to an increase of sodium dependent sugar transport due to an augmented amount of SGLT1 localized in the plasma membrane [Hirsch et al., 1996]. Thus, SGLT1 sorting between the intracellular compartments and the plasma membrane, which occurs by exo- and endocytosis [Wright et al., 1992; Kipp et al., 2003; Khoursandi et al., 2004] is affected. The

Abbreviations used: AMG, [^{14}C]-α-methyl-D-glucopyranoside; CHO-G6D3, Chinese hamster ovary cells stably expressing rabbit SGLT1; CHO, Chinese hamster ovary cells; DAPI, 4'-6-diamidine-2-phenylindol; Cyt-D, cytochalasin D; DMEM, Dulbecco's modified Eagle's medium; EZ-Link Sulpho-NHS-SS-Biotin, sulfosuccinimidyl 2-(biotinamido)-ethyl-1, 3-dithiopropionate; H-89, N-(2-((*p*-bromo-cinnamyl) amino) ethyl)-5-isoquiniline sulphonamide HCl; HEPES, 4-(2-hydroxyethyl)-1-piperazineethanesulfonic acid; KRH, Krebs-Ringer-HEPES medium; K_{SV}, collisional quenching constant; NMG, *N*-methylglucamine; PBS, phosphate buffered saline; PKA, protein kinase A; RIPA, radioimmunoprecipitation buffer assay SGLT1, Na^+/D-glucose co-transporter; TBS, tris buffered saline; Trp, tryptophan; SDS–PAGE, sodium dodecylsulfate–polyacrylamide gel electrophoresis; 8-Br-cAMP, 8-bromo adenosine 3′, 5′-cyclic monophosphate.

*Correspondence to: Dr. Francisco Castaneda, Laboratory for Molecular Pathobiochemistry and Clinical Research, Max Planck Institute of Molecular Physiology, Otto-Hahn-Strasse 11, 44227 Dortmund, Germany.
E-mail: francisco.castaneda@mpi-dortmund.mpg.de

Received 23 May 2008; Accepted 19 November 2008 • DOI 10.1002/jcb.22025 • 2008 Wiley-Liss, Inc.
Published online 29 December 2008 in Wiley InterScience (www.interscience.wiley.com).

important role of transport trafficking has been corroborated in human intestinal Caco-2 cells, a model for human enterocytes [Kipp et al., 2003; Khoursandi et al., 2004]. In these cells a large intracellular pool of SGLT1 is found, which is part of a regulatory mechanism whereby sodium-dependent sugar uptake at the cell surface can be altered.

Interestingly, in former studies a direct effect of PKA on SGLT1 was not observed. However, based on the consensus sites for phosphorylation by protein kinases found in rabbit and human SGLT1 [Wright et al., 1992, 1997], namely Ser418, the possibility of a direct transporter modulation through phosphorylation induced by PKA can be postulated. As a consequence, further regulatory processes in the regulation of SGLT1-mediated transport, in addition to distribution of SGLT1 between the apical membrane and intracellular compartments, can be imagined.

The expression and isolation hSGLT1 from a heterologous expression system offers the possibility to study a possible direct effect of phosphorylation on the conformation of the molecule [Tyagi et al., 2005]. Changes of conformation have recently been analyzed in this system and correlated to different functional states of the transporter [Kumar et al., 2007a,b].

Therefore, the aim of the present study was to investigate the role of PKA on the regulation of SGLT1 activity in vivo and to correlate it with the conformation of recombinant human hSGLT1 in vitro.

MATERIALS AND METHODS

DRUGS AND REAGENTS

All chemicals were of the highest purity available from Sigma (Deisenhofen, Germany) unless other sources are indicated. Forskolin, 8-Br-cAMP and protein kinase A (PKA; catalytic subunit, bovine heart) were obtained from Calbiochem (Darmstadt, Germany). [^{14}C]α-methyl D-glucopyranoside ([^{14}C]-AMG; specific radioactivity 300mCi/mmol), [^{32}P] adenosine 5′ triphosphate ([^{32}P]-ATP; specific radioactivity 3,000 Ci/mmol) were purchased from Perkin–Elmer (Boston, MA). Cy-3 conjugated goat anti-rabbit IgG was purchased from Dianova (Hamburg, Germany). For immunobloting, anti SGLT1 antibody (QIS 30), a Glutathione-S-transferase fusion protein containing the extracellular fragment of rabbit SGLT1 (amino acids 243–272, starting with Q, I, S), was used [Kipp et al., 2003].

CELL CULTURE AND TRANSFECTION

Chinese hamster ovary cells stably expressing rbSGLT1 (CHO-G6D3) generated in our laboratory [Lin et al., 1998] were grown in 25-cm^2 flasks (Falcon, Heidelberg, Germany) under 7.5% CO_2 at 37°C. The cells were cultured to 80% confluence in DMEM (PAN Biotech, Aidenbach, Germany) containing low glucose (5 mM) supplemented with 5% fetal calf serum, 1 mM sodium pyruvate, 2 mM glutamine and 50 μM β-mercaptoethanol and 400 μg/ml paneticin G420. For transient expression of wild-type rbSGLT1 and Ser418Ala mutant rbSGLT1, CHO cells grown in 24-well plates (5% CO_2 at 37°C) in DMEM supplemented with 10% fetal calf serum, 2 mM glutamine and transfected using Superfect Transfection Kit (Qiagen, Hilden, Germany) according to the manufacturer's protocol were used.

[^{14}C] α- METHYL-D-GLUCOPYRANOSIDE (AMG) UPTAKE

Sodium dependent D-glucose co-transport activity in CHO-G6D3 and CHO (wild-type rbSGLT1 or Ser418Ala mutant rbSGLT1) cells was determined by measuring the uptake of α-methyl-D-glucopyranoside (AMG), a substrate specific for SGLT1. Cells were grown to confluence in 24-well plates at a concentration of 2×10^4 cells/well and maintained in culture for 2 days to allow the cells to form a confluent monolayer [Castaneda and Kinne, 2005]. Prior to the transport assay, the cells were incubated in a D-glucose free medium for 2 h at 37°C to remove the extracellular D-glucose and to reduce the intracellular glucose concentration [Lin et al., 1998]. For the purpose of this study, Krebs-Ringer-Henseleit (KRH) solution containing 120 mM NaCl, 4.7 mM KCl, 1.2 mM $MgCl_2$, 2.2 mM $CaCl_2$, 10 mM Hepes (pH 7.4 with Tris) was used to assess sodium-dependent D-glucose transport. For sodium-free conditions, KRH solution containing 120 mM *N*-methyl-glucamine (NMG) instead of NaCl (Na^+) was used.

Briefly, cells with pre-treated the indicated drugs for 15 min at 37°C were incubated for 30 min with 500 μl transport buffer containing KRH-Na^+ or KRH-NMG plus [^{14}C]AMG (0.1 μCi/μl). At the end of the uptake period 500 μl of ice-cold stop buffer (KRH-Na^+, containing 0.5 mM phlorizin) was added. Then, cells were solubilized in 2% SDS, the amount of radioactive AMG taken up was counted and then protein content determined as described by Bradford [1976]. Finally, sodium-dependent uptake was calculated by subtracting the uptake values obtained in absence of sodium (KRH-NMG) from the values of KRH-sodium and expressed as pmol/mg protein/30 min.

KINETIC STUDIES

The kinetic constants (K_m and V_{max}) of the sodium-dependent AMG uptake were determined by non-linear regression analysis, using GraphPad Prism Software version 5.01. For that purpose, seven substrate concentrations (AMG 3–20 μM) were used in the presence of forskolin (1 μM for 15 min) and in absence of forskolin (control group). Sodium-dependent AMG uptake was measured as described above.

MEMBRANE PREPARATION

CHO-G6D3 cells grown in Petri dishes were treated with PKA activators forskolin (1 μM) and 8-Br-cAMP (100 μM) for 15 min at 37°C. Then, the cells were scraped from the plates and centrifuged at 500*g* for 10 min at 4°C. The pellet was suspended in 1 ml of ice-cold hypotonic buffer (10 mM HEPES-Tris, 5 mM EGTA-Na^+ and 0.01% thimerosal, pH 7.4) supplemented with protease and phosphatase inhibitors. The cells were lysed by two freeze-thaw cycles and centrifuged at 100,000*g* for 60 min at 4°C to remove the cytosolic proteins. Then, the pellets were solubilized in hypotonic buffer containing 1% Triton X-100 and incubated at 4°C for 30 min. The non-solubilized material was centrifuged again to exclude the non-solubilized material. The supernatants, which represent the membrane protein fraction, were analyzed by Western blotting with the anti-SGLT1 antibody QIS-30 (1:1,000). The quantification of the rbSGLT1 amount was performed by using ImageJ v. 1.34 software for Windows (National Institutes of Health, Bethesda, Bethesda, USA) using the integrated optical density of bands and expressed as

fold-values of the average optical density of untreated, control CHO cells.

CELL SURFACE BIOTINYLATION

Biotinylation of cell surface proteins was performed on CHO-G6D3 cells grown in Petri dishes treated with 1 μM forskolin and 100 μM 8-Br-cAMP for 15 min at 37°C. Then, the CHO-G6D3 cells were incubated with in 0.5 mg/ml EZ-Link Sulpho-NHS-SS-Biotin (Pierce, Rockford, IL) in PBS (pH 8.0) for 30 min at 4°C. Then, cells were incubated for 40 min at 4°C in quenching solution (100 mM glycine in PBS; pH 8.0) to stop cell biotinylation. Then the cells were lysed with radioimmunoprecipitation buffer assay (RIPA) buffer (150 mM NaCl, 0.1% SDS, 0.5% sodium desoxycholate, 1% Triton X-100; pH 7.4), supplemented with protease and phosphatase inhibitors for 1 h at 4°C and centrifuged at 14,000*g* for 10 min at 4°C. The lysates were incubated with 100 μl of streptavidin beads overnight at 4°C. The pellets were washed three times with cold RIPA buffer, resuspended in 50 μl of Laemmli sample buffer (60 mM Tris–HCl, pH 6.8, 25% glycerol, 2% SDS, 14.4 mM 2-β-mercaptoethanol and 0.1% bromophenol blue) and centrifuged at 14,000*g* for 10 min at 4°C. The resulting supernatant (the biotinylated fraction) was separated by SDS–PAGE and immunoblotted with the anti-SGLT1 antibody (QIS 30, 1:500).

ANTI-PHOSPHOPEPTIDE ANTIBODY (p-Ser418)

A polyclonal anti-peptide antibody for serine 418, corresponding to amino acids 413–424 (CVRKRASEKELMI), was synthesized by Eurogentec (Seraing, Belgium) in rabbits immunized with the keyhole-limpet hemocyanin-conjugated peptide. The sera from the rabbit were first purified by negative affinity purification by incubating the sera on a Sepharose column in which the corresponding non-phosphorylated peptide was covalently bound. For subsequent positive purification, the flow-through fractions were collected and then loaded on a second column in which the phosphorylated peptide was covalently bound and eluted with 100 mM glycine (pH 2.5). The antibodies were dialyzed into PBS with 0.01% thimerosal and 0.1% BSA.

CONSTRUCTION OF PKA SITE MUTANT BY SITE-DIRECTED MUTAGENESIS

The PKA mutant was prepared by site-directed mutagenesis using Quickchange kit (Stratagene, La Jolla, CA). For this purpose the pEGFP C-1 Gateway expression vector containing the Ser418Ala mutant rbSGLT1 cDNA was used as template and subcloned into pHook-2. Polymerase chain reaction was used to generate restriction sites at the ends of insert DNA and digested with *Hind*III and *Nhe*I restriction enzymes (NEB, Frankfurt, Germany) followed by ligation to pHook-2. The sequence of mutant cDNA was confirmed by DNA sequencing (Applied Biosystems, Darmstadt, Germany).

PHOSPHORYLATION ASSAY

Purified, recombinant hSGLT1 (~10 μg) synthesized in our laboratory [Tyagi et al., 2005] was used for the phosphorylation assay. For this purpose, a reaction volume of 50 μl containing 40 mM HEPES (pH 7.0), 20 mM $MgCl_2$, and 57 ng of the catalytic subunit of PKA was used. The reaction was initiated by adding 0.1 mM ATP containing 3 μCi of [^{32}P] ATP and continued for 60 min at 30°C. The reaction was terminated by the addition of SDS-sample buffer (60 mM Tris–HCl, pH 6.8, 25% glycerol, 2% SDS, 14.4 mM 2-β-mercaptoethanol, and 0.1% bromophenol blue). The samples were then electrophoresed, Coomassie stained and visualized by autoradiography. For control experiments, the conditions were the same as the phosphorylation assay except that PKA or the purified protein was omitted. The stoichiometry of the phosphorylation was determined by measuring the amount of [^{32}P] incorporated in the transporter. For this purpose, a duplicate gel was stained with Coomassie and the protein bands were cut out and incubated in Solvable (500 μl at 50°C for 3 hrs). At the end of the incubation period 7 ml of the Ultima Gold scintillation solution (Perkin–Elmer) was added and the samples were counted.

STEADY STATE TRYPTOPHAN FLUORESCENCE AND ACRYLAMIDE-DEPENDENT TRYPTOPHAN FLUORESCENCE QUENCHING

Steady state tryptophan (Trp) fluorescence measurements were performed as described previously [Raja et al., 2003]. Purified, recombinant hSGLT1 (~20 μg) in PBS (pH 7.4) was incubated in the presence or absence of PKA or ATP (1 mM) and/or D-glucose (5 mM) at room temperature for 5 min prior to collecting the fluorescence spectra. The excitation wavelength was set to 295 nm for selective excitation of Trp fluorescence. Emission spectra between 300 and 400 nm were averaged from eight different scans. In addition, acrylamide-dependent Trp fluorescence quenching experiments were performed using increasing concentrations of the hydrophilic collisional quencher acrylamide (50–700 mM). The accessibility of Trp was monitored by analyzing the quenching data according to the Stern-Volmer equation: $F_0/F = 1 + K_{SV}$ [Q]; where F and F_0 represent the fluorescence intensities in the presence and absence of acrylamide, respectively, [Q] is the concentration of quenching agent, and K_{SV} is the Stern-Volmer quenching constant [Prince et al., 1993]. In the case of a purely collisional quenching mechanism, a Stern-Volmer plot of F_0/F versus [Q] gives a linear plot with a slope equal to K_{SV}.

STATISTICAL ANALYSIS

The data are given as mean ± standard error (SE) from a number (n) of independent experiments. Statistical comparisons between treated versus untreated (control) cells were performed by independent *t*-test analysis. *P* values less than 0.05 (two tailed) were considered statistically significant.

RESULTS

PKA ACTIVATION STIMULATES AMG UPTAKE IN CHO-G6D3 CELLS

As shown in Figure 1A, sodium-dependent AMG uptake had mean values of 1,861 ± 99 pmol/mg protein/30 min after forskolin treatment (1 μM for 15 min at 37°C) or values of 1,676 ± 108 pmol/mg protein/30 min after 8-Br-cAMP treatment (100 μM for 15 min at 37°C). These values were significantly higher when compared to untreated, control cells ($^*P < 0.01$; n = 16) in which values of 1,156 ± 117 pmol/mg protein/30 min were found. These data

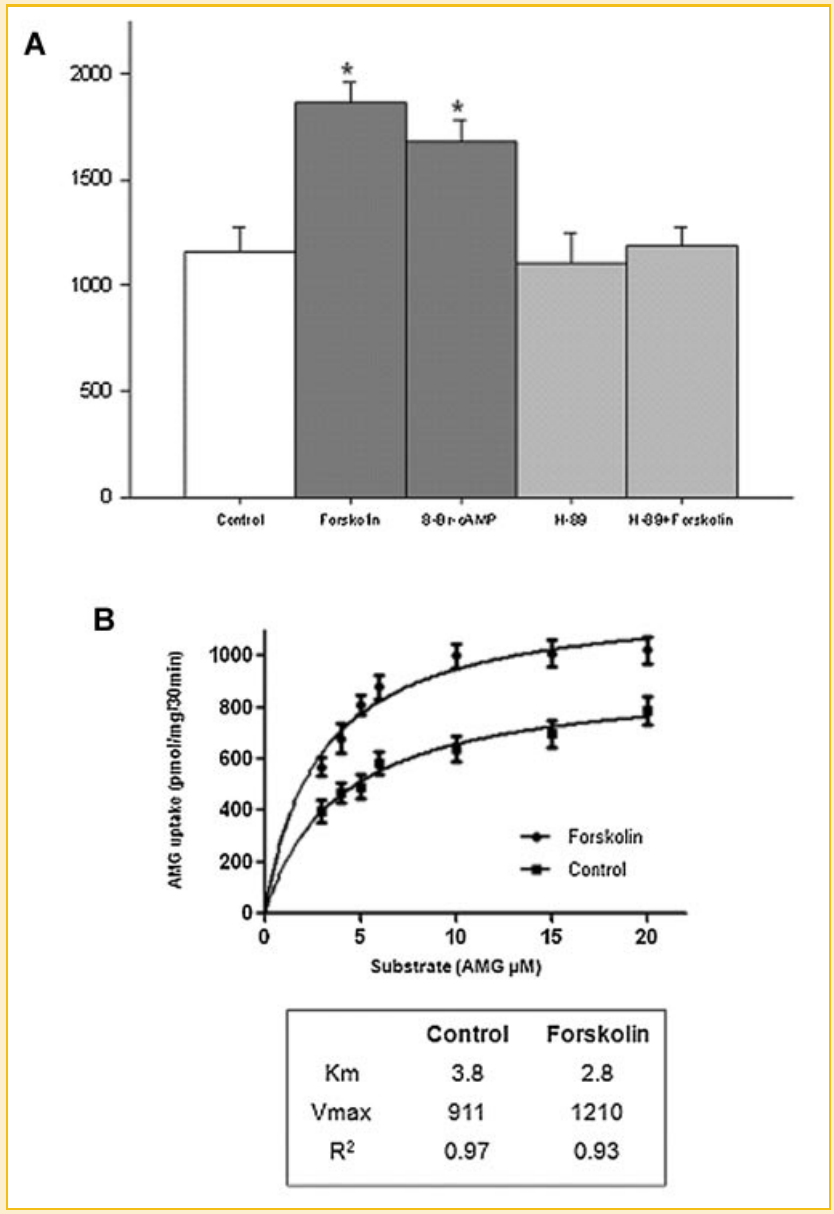

Fig. 1. Effect of PKA activators and inhibitors on sodium-dependent AMG uptake in CHO-G6D3 cells. A: Cells were preincubated at 37°C with forskolin (1 μM), 8-Br-cAMP (100 μM), H-89 (10 μM) or H-89 (10 μM) + forskolin (1 μM) for 15 min prior to uptake experiments and compared to untreated CHO-G6D3 cells (control). The chemical concentration of AMG was 3 μM. AMG uptake was measured after 30 min at 37°C in the presence or absence of the compounds indicated. Results are mean ± SE, n = 16. *$P < 0.01$ treated versus untreated, control cells. B: Kinetic analysis (K_m and V_{max}) of the degree of PKA-stimulated phosphorylation on rbSGTL1 treated with forskolin and 8-Br-cAMP was determined by AMG uptake. Additionally, non-linear regression analysis in treated and control CHO-G6D3 cells was carried out to determine the relationship between AMG substrate and uptake values in the presence or absence of forskolin.

represent an increase in sodium-dependent AMG uptake equivalent to 61% and 45% after forskolin and 8-Br-cAMP treatment, respectively. To corroborate that the stimulatory effect resulted from the activation of PKA, CHO-G6D3 cells were pretreated with the PKA inhibitor H-89 (10 μM for 15 min at 37°C). H-89 pretreatment resulted in a sodium-dependent AMG uptake of 1,098 ± 151 pmol/mg protein/30 min, which is similar to the basal sodium-dependent AMG-uptake found in CHO-G6D3 cells (Fig. 1A). In addition, H-89 completely abolished the stimulatory effect of forskolin on SGLT1-mediated AMG uptake, as shown by values of 1,190 ± 86 pmol/mg protein/30 min. This uptake level was similar to that seen in the case of untreated, control cells.

To analyze further the effect of PKA activation on sodium-dependent AMG uptake, kinetic studies after forskolin treatment were performed. As shown in Figure 1B, sodium-dependent AMG uptake without forskolin (control) had a K_m value of 3.8 μM. This value was higher than the value of 2.8 μM obtained after forskolin treatment (1 μM for 15 min). The V_{max} for control, untreated cells was 911 pmol/mg protein/30 min, which was lower than the V_{max} found in forskolin treated cells with a value of 1,210 pmol/mg

protein/30 min. We also found significant positive associations between AMG substrate and uptake values in the presence ($R^2 = 0.93$, $P < 0.01$) and absence ($R^2 = 0.97$, $P < 0.01$) of forskolin.

PKA ACTIVATION INCREASES THE AMOUNT OF SGLT1 IN THE PLASMA MEMBRANE

The effect of forskolin on the amount of rbSGLT1 in the plasma membrane is shown in Figure 2. Figure 2A shows representative microscopic images of the immunostaining analysis. The effect of increasing intracellular levels of cAMP in CHO-G6D3 cells treated with forskolin (1 μM) plus 8-Br-cAMP (100 μM) caused a slight increase in the distribution of SGLT1 labeled with the anti-SGLT1 antibody, QIS-30, as compared to untreated, control cells. To be able to quantify this effect Western blot analysis of the cell membrane fraction was performed (Fig. 2B). The amount of rbSGLT1 blotted from plasma membrane fraction in CHO-G6D3 cells treated with combined forskolin and 8-Br-cAMP was higher than in the untreated, control cells ($^*P < 0.05$; n = 6), as shown by an integrated density of 3.2 ± 0.2 and 2.7 ± 0.2 arbitrary units, respectively. As also shown in Figure 2B, the amount of rbSGLT1 blotted from the biotinylated fraction in CHO-G6D3 cells treated with forskolin plus 8-Br-cAMP was slightly higher than in the untreated, control cells ($^*P < 0.05$; n = 6), as shown by an integrated density of 2.8 ± 0.2 and 2.5 ± 0.3 arbitrary units found in each cell group, respectively.

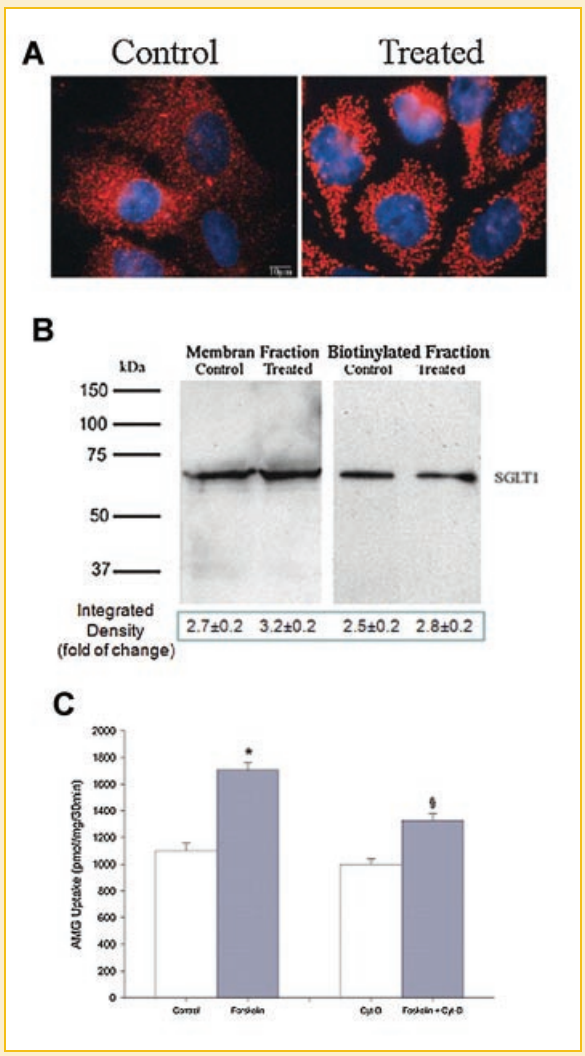

Fig. 2. Effect of PKA activators on the amount of SGLT1 in the plasma membrane. A: Representative immunostaining images for rbSGLT1 in CHO-G6D3 cells treated with the combination of PKA activators (forskolin at 1 μM and 8-Br-cAMP at 100 μM for 15 min at 37°C) compared to untreated, control cells. B: Plasma membrane and biotinylated fractions from both treated and untreated, control cells (20 μg protein/lane) blotted with an anti-SGLT1 antibody (QIS-30; 1:1,000) with quantitative analysis of the blotted rbSGLT1 using the integrated optical density of bands and expressed as arbitrary units of the average optical density of CHO cells. Values are mean ± SE, n = 6. $^*P < 0.05$ treated versus untreated, control CHO cells. C: Effect of cytochalasin D (Cyt-D) on forskolin-induced AMG uptake in CHOG6D3 cells. Results are mean ± SE, n = 24. $^*P < 0.01$ treated versus untreated, control cells or $^§P < 0.01$ treated versus cytochalasin D without forskolin.

To further evaluate the effect of PKA activation on the insertion of additional transporters into the plasma membrane through membrane trafficking, the effect of cytochalasin D, an actin filament disruptor, was determined. As shown in Figure 2C, in the absence of cytochalasin D (Cyt-D), forskolin stimulates the transport activity of G6D3 cells to $1{,}706 \pm 52$ pmol/mg protein/30 min ($^*P < 0.01$; n = 24) as compared to untreated, control cells ($1{,}099 \pm 57$ pmol/mg protein/30 min). This result represents an increase in sodium-dependent AMG uptake equivalent to 55%. In contrast, in pretreated cytochalasin D cells the effect of forskolin (forskolin + Cyt-D) was slightly reduced, as shown by uptake values of $1{,}328 \pm 48$ pmol/mg protein/30 min ($^§P < 0.01$; n = 24) as compared to cytochalasin D pretreated cells without forskolin (999 ± 40 pmol/mg protein/30 min), which represents a reduction of the effect of forskolin in sodium-dependent AMG uptake equivalent to 25%, while 30% of the effect of forskolin remains present. These data suggest additional mechanisms that stimulate AMG-uptake.

REMOVAL OF THE PUTATIVE PKA SITE ON SGLT1 ATTENUATES THE STIMULATION OF AMG-UPTAKE

As shown in Figure 3, forskolin and 8-Br-cAMP stimulated the sodium-dependent AMG uptake in CHO cells transiently expressing wild type rbSGLT1 by a mean value of 621 ± 16 pmol/mg protein/30 min ($^*P < 0.01$; n = 24) and 492 ± 34 pmol/mg protein/30 min ($^*P < 0.01$; n = 24); respectively, untreated control cells had a value of 318 ± 40 pmol/mg protein/30 min. Interestingly, in cells transfected with the Ser418Ala mutant rbSGLT1 the stimulation by PKA activation of the sodium-dependent AMG uptake was still observed, albeit to a lesser extent, as shown by mean values of 468 ± 35 pmol/mg protein/30 min ($^*P < 0.01$; n = 24) or 382 ± 24 pmol/mg protein/30 min ($^*P < 0.01$; n = 24), after forskolin or 8-Br-cAMP stimulation, respectively. These values were significantly higher than those obtained in untreated, mutant cells (315 ± 27 pmol/mg protein/30 min ($^*P < 0.01$; n = 24)). They are, however, by 25% and 22% significantly lower than those found in the corresponding wild-type CHO cells ($^§P < 0.05$).

Thus part of the stimulation of the sodium-dependent D-glucose uptake by PKA activation appeared to be direct, that is, depending on the phosphorylation of SGLT1.

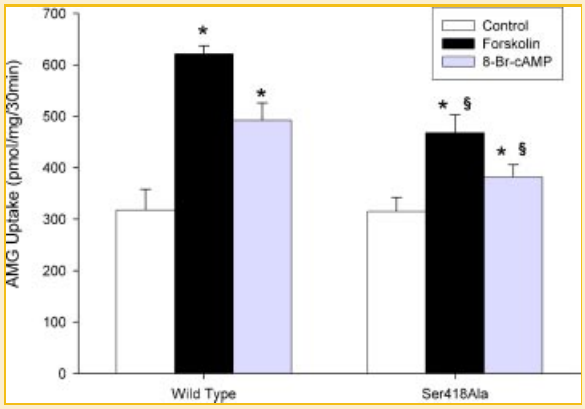

Fig. 3. Effect of mutation of PKA consensus site on AMG uptake. Wild-type and Ser418Ala mutant rbSGLT1 transiently transfected CHO cells were treated for 15 min with forskolin (1 μM) or 8-Br-cAMP (100 μM) at 37°C. AMG uptake was measured after 30 min in the absence or presence of the indicated compounds. Values are mean ± SE, n = 24. $^{*}P < 0.01$ treated versus untreated, control CHO cells; $^{\S}P < 0.05$ versus wild-type CHO cells. [Color figure can be viewed in the online issue, which is available at www.interscience.wiley.com.]

EFFECT OF PKA ACTIVATION ON PHOSPHORYLATION OF rbSGLT1 IN VIVO

As shown in Figure 4, after forskolin and 8-Br-cAMP-treatment the amount of phosphorylated rbSGLT1 was significantly increased ($^{*}P < 0.05$; n = 12). This is evident from an integrated density of 11.4 ± 0.6 arbitrary units as compared to untreated control CHO-G6D3 cells in which an integrated density of 2.1 ± 0.3 arbitrary units was found. The specificity of the phospho-S418 antibody was demonstrated with recombinant hSGLT1 (Fig. 4). The phospho-S418 antibody detects a protein of approximately 55 kDa representing the non-glycosylated hSGLT1 only in the phosphorylated state.

RECOMBINANT hSGLT1 ACTS AS SUBSTRATE FOR PKA IN VITRO

To investigate whether SGLT1 served as a substrate for PKA, recombinant hSGLT1 was incubated with the catalytic subunit of PKA in the presence of [^{32}P] ATP. As shown in Figure 5A, an autoradiography signal corresponding to hSGLT1 with the expected apparent molecular mass of ~55 kDa was observed in the presence of PKA. In contrast, no autoradiography signal was detected on hSGLT1 when PKA was omitted. The observed additional band at ~40 kDa represents the autophosphorylated form of PKA. A Coomassie stained gel corroborates the presence of the protein (Fig. 5B). The stoichiometry of phosphorylation of hSGLT1 by PKA was determined by measuring the amount of ^{32}P incorporated in the protein (Fig. 5C). We found a phosphorylation stoichiometry of 1.05 ± 0.02 mol phosphate/mole SGLT1 in the presence of PKA compared to an incorporation of 0.045 ± 0.01 mol phosphate/mole SGLT1 in its absence.

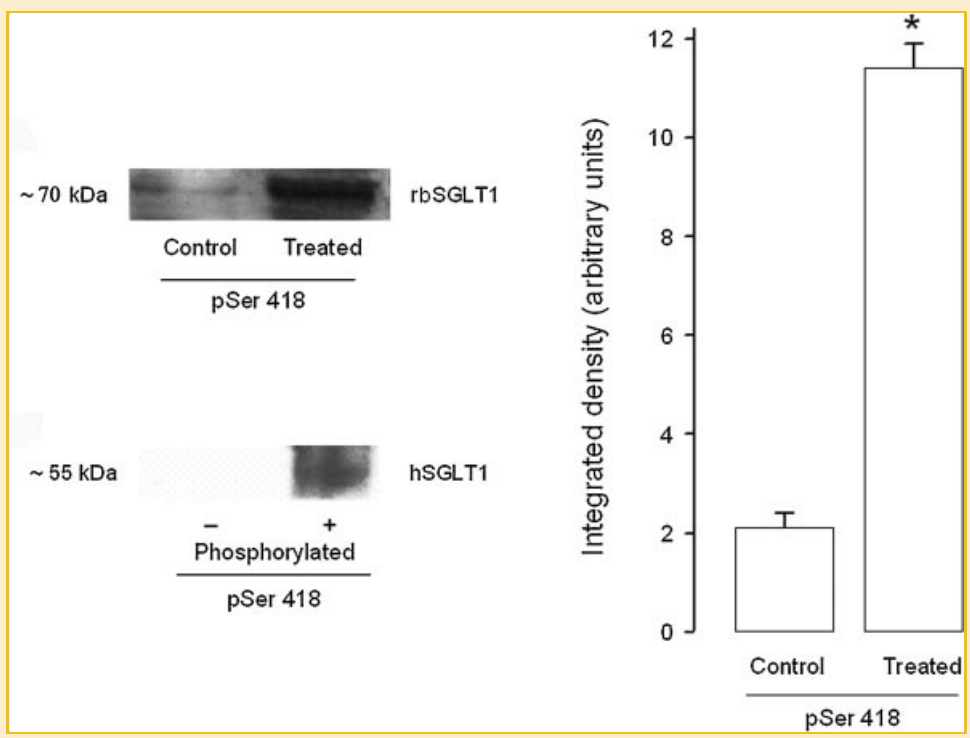

Fig. 4. Extent of phosphorylation of rbSGLT1 induced by PKA. A: Representative Western blot for phosphorylated and non-phosphorylated rbSGLT1 in cell membrane preparations following incubation of CHO-G6D3 cells with the combination of PKA activators (forskolin at 1 μM and 8-Br-cAMP at 100 μM) for 15 min at 37°C. Membrane fractions from both treated and untreated (control) cells were blotted with an anti-phosphopeptide antibody p-Ser418 (p-Ser 418; 1:50) and quantified by analysis of the phosphorylated rbSGLT1, using the integrated optical density of bands and expressed as arbitrary units of the average optical density of CHO cells. Values are mean ± SE, n = 12. $^{*}P < 0.05$ treated versus untreated, control CHO cells.

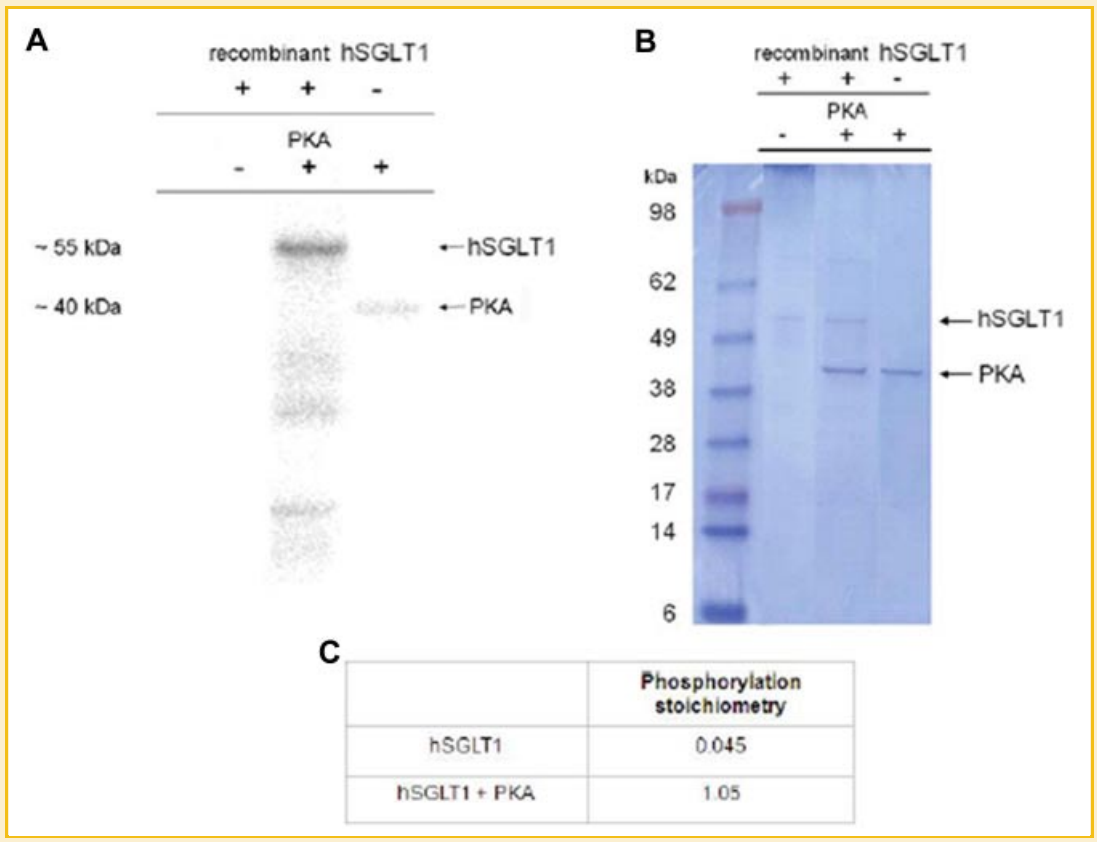

Fig. 5. Effect of PKA on phosphorylation of recombinant human hSGLT1. A: Representative autoradiography of in vitro phosphorylation of recombinant hSGLT1 induced by PKA demonstrates the effect of PKA phosphorylation on hSGLT1. Purified hSGLT1 was incubated with the catalytic subunit of PKA in a buffer containing [^{32}P]ATP. An autoradiography signal was visible at ~55 kDa, indicating that hSGLT1 is phosphorylated by PKA. No signal was detected in hSGLT1control cells in which PKA or [^{32}P] ATP were omitted. B: Coomassie stained gel corroborating the presence of the protein. C: Phosphorylation stoichiometry data of hSGLT1. [Color figure can be viewed in the online issue, which is available at www.interscience.wiley.com.]

PHOSPHORYLATION INDUCES CONFORMATIONAL CHANGES OF hSGLT1

As shown in Figure 6A the corrected tryptophan fluorescence emission spectra (excitation wavelength at 295 nm) of both non-phosphorylated and phosphorylated hSGLT1 in vitro depicted a maximum emission at 343 nm. Phosphorylated hSGLT1 had ~20% less fluorescence intensity compared to non-phosphorylated hSGLT1. Phosphorylated hSGLT1 showed also a significant increase in the accessibility of the Trps to the hydrophilic quencher acrylamide, $KSV = 1.45 \pm 0.05\ M^{-1}$ compared to $1.02 \pm 0.02\ M^{-1}$ ($^{*}P < 0.05$; $n = 12$) in the control. As shown in Figure 6B, the fluorescence emission intensity of both phosphorylated and non-phosphorylated hSGLT1 was increased by D-glucose. This is shown by fluorescence intensities of 255 and 325 nm, respectively. In addition, phosphorylated hSGLT1 exhibited the highest accessibility of Trps to acrylamide. The phosphorylation resulted in an increase in the K_{SV} values from $1.24 \pm 0.05\ M^{-1}$ to $1.91 \pm 0.04\ M^{-1}$ ($^{*}P < 0.01$; $n = 12$).

DISCUSSION

In the present study we analyzed the effect of PKA on the regulation of sodium-sugar-cotransport (SGLT) at two different levels of complexity: in vivo in a cellular system expressing rabbit SGLT1 (rbSGLT1), and in vitro on isolated recombinant human SGLT (hSGLT1) protein. In the cellular system we observed an increase in transport activity after stimulation of PKA by forskolin or 8-Br-cAMP. The increase in transport activity was associated with an increased amount of rbSGLT1 localized in the plasma membrane. Furthermore, we found a direct effect of PKA mediated phosphorylation on the conformation of hSGLT1.

The effect of increased intracellular cAMP on the sorting of the transporter was expected based on previous reports using oocytes [Hirsch et al., 1996; Wright et al., 1997] and rat jejunal brush border [Ishikawa et al., 1997]. An increased amount of SGLT1 localized into the plasma membrane was deduced in the former studies based on the increase in V_{max}, in the surface areas of the oocytes or an increase in the number of phlorizin binding sites. In the current study also an increase in V_{max} was observed. In addition, immunohistochemistry and surface biotinylation demonstrated a higher presence of the transporter in the cell membrane. Furthermore, disruption actin filaments induced by cytochalasin D reduced the stimulation of AMG uptake by forskolin. These results underline the importance of the regulation of glucose uptake activity by changes of SGLT1 trafficking to the plasma membrane through exo- and endocytosis [Khoursandi et al., 2004].

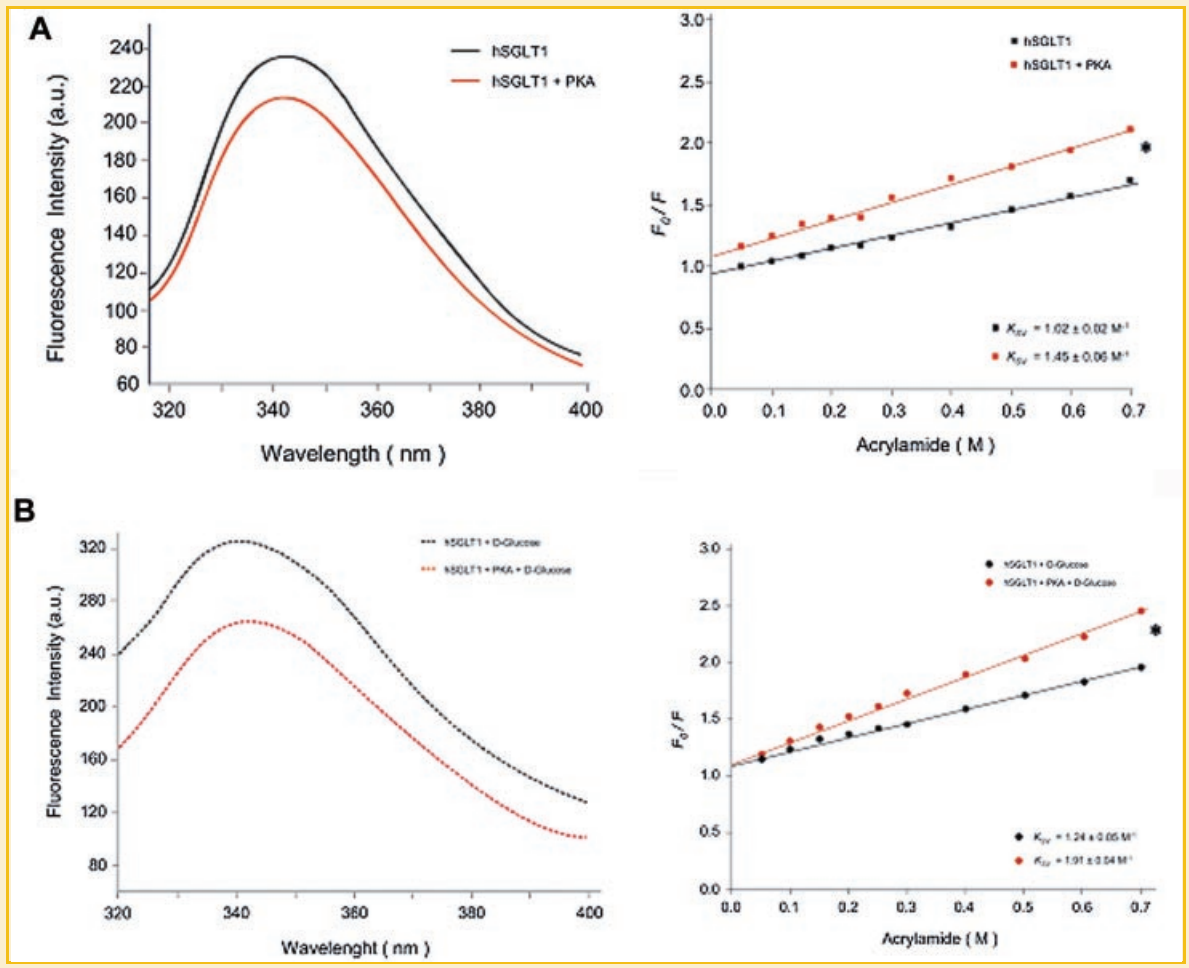

Fig. 6. A: Effect of PKA phosphorylation on conformational changes of hSGLT1 assessed by steady state tryptophan fluorescence measurements (emission spectra and quenching by acrylamide). B: Effect of PKA phosphorylation on conformational changes of hSGLT1 in the presence and absence of D-glucose. Fluorescence intensity was represented in arbitrary units and data on fluorescence quenching by acrylamide were calculated according to the Stern-Volmer equation (K_{SV}). Values are mean ± SE, n = 12. $^*P < 0.05$ phosphorylated versus non-phosphorylated hSGLT1.

The lack of complete abolition of the forskolin effect by cytochalasin D suggested that factors additional to the stimulus-dependent insertion of SGLT1 into the plasma membrane had to be considered. The assumption of a complementary regulatory mechanism of PKA on sodium-dependent AMG uptake was confirmed by the results obtained in Ser418Ala mutant cells stimulated by forskolin or by 8-Br-cAMP, which showed that stimulation of sodium-dependent AMG uptake, at least partly, required the presence of the putative PKA site of rbSGLT1. Indeed the extent of phosphorylation of rbSGLT1 increased in the presence of PKA activators as evident from the Western blots using the anti-phosphopeptide antibody. A direct effect of PKA phosphorylation on the activity of SGLT1 has also been reported in the rat small intestine, in which the physiological relevance of PKA-mediated phosphorylation of SGLT1 has been shown [Ishikawa et al., 1997]. The direct regulatory mechanism of PKA on SGLT1 activity through phosphorylation of the transporter was also supported by the finding of an increase of the affinity of AMG transport by forskolin.

In the present study, we also found conformational changes in hSGLT1 induced by PKA phosphorylation, which indicate that PKA phosphorylation may be a complementary mechanism involved in the regulation of SGLT1-mediated glucose transport. Tryptophan fluorescence is widely used as a tool to monitor changes in proteins and to make inferences regarding local structure and dynamics [Vivian and Callis, 2001]. The emission spectra obtained by non-phosphorylated SGLT1 indicated that most of the Trp is buried within the protein. This is in accordance with topology predictions of SGLT1 in which most of the Trps are located in a hydrophobic environment, and corroborates our previous findings on Trp localization [Raja et al., 2003; Kumar et al., 2007b]. In addition, acrylamide quenching experiments provided valuable information regarding the conformational changes of proteins, in this case SGLT1. The acrylamide quenching experiments suggest that phosphorylation induces a conformational change of hSGLT1 allowing for some of the Trps to become more surface-exposed, and hence more easily quenched by acrylamide. This was seen by the

changes in the Stern-Volmer constant (K_{SV}) we found. Similar observations were reported for the cystic fibrosis transmembrane conductance regulator (CFTR) where phosphorylation led to increased accessibility to acrylamide [Johnson and Lewis, 2001; Grimard et al., 2004].

D-glucose increased the emission intensity of both non-phosphorylated SGLT1 as well of phosphorylated SGLT1. In addition, the phosphorylated SGLT1-glucose complex showed the highest Stern-Volmer constant and the highest accessibility of Trp to acrylamide. A similar observation was reported for phenylalanine hydroxylase, in which phosphorylation of Ser16 by PKA induced a conformational change between Arg13/Lys14 resulting in a more accessible active site [Miranda et al., 2002, 2004]. It is also known that the addition of a phosphoryl group to Ser, Thr, or Tyr residues can have a profound effect on protein conformation by facilitating the formation of electrostatic interactions between the phosphate group and the side chain of Arg or Lys [Johnson and Lewis, 2001]. Whether and how the conformational changes observed in the isolated carrier bring about the change in affinity of the transporter observed in the intact cells remains to be elucidated. By transferring the results on the isolated protein to the complex cellular level one also has to consider the species differences—in the intact cells rbSGLT1, in the cuvette hSGLT1 was studied. Since both reacted similar to PKA activation when expressed in oocytes we currently assume that such inference is warranted.

In conclusion, the present study demonstrates that activation of PKA stimulates the SGLT1-mediated uptake of sugars into CHO cells. This effect is due to an indirect and direct effect of PKA on SGLT1. The indirect effect concerns a change in the sorting of the transporter between intracellular compartments and the plasma membrane, which results in an increased number of transporters in the plasma membrane. The direct effect involves phosphorylation of the SGLT1 at the PKA consensus site. The phosphorylation induces conformational changes which alter the functional properties of the transporter. This new information points to an important complementary mechanism in the regulation of SGLT1-mediated glucose transport in epithelial cells which should be investigated further.

ACKNOWLEDGMENTS

We gratefully acknowledge the excellent technical assistance of Christiane Pfaff, Jutta Luig, Hendrike Schütz and Kirsten Michel. Navneet Tyagi provided us with purified recombinant hSGLT1. We also acknowledge the financial support of the International Max Planck Research School in Chemical Biology, Dortmund, Germany.

REFERENCES

Bradford MM. 1976. A rapid and sensitive method for the quantitation of microgram quantities of protein utilizing the principle of protein-dye binding. Anal Biochem 72:248–254.

Castaneda F, Kinne RKH. 2005. A 96-well automated method to study inhibitors of human sodium-dependent D-glucose transport. Mol Cell Biochem 280:91–98.

Grimard V, Li C, Ramajeesingh M, Bear CE, Goormaghtigh E, Ruysschaert JM. 2004. Phosphorylation-induced conformational changes of cystic fibrosis transmembrane conductance regulator monitored by attenuated total reflection-Fourier transform IR spectroscopy and fluorescence spectroscopy. J Biol Chem 279:5528–5536.

Hirsch JR, Loo DD, Wright EM. 1996. Regulation of Na+/glucose cotransporter expression by protein kinases in Xenopus laevis oocytes. J Biol Chem 271:14740–14746.

Ishikawa Y, Eguchi T, Ishida H. 1997. Mechanism of beta-adrenergic agonist-induced transmural transport of glucose in rat small intestine. Regulation of phosphorylation of SGLT1 controls the function. Biochim Biophys Acta 1357:306–318.

Johnson LN, Lewis RJ. 2001. Structural basis for control by phosphorylation. Chem Rev 101:2209–2242.

Khoursandi S, Scharlau D, Herter P, Kuhnen C, Martin D, Kinne RK, Kipp H. 2004. Different modes of sodium-D-glucose cotransporter-mediated D-glucose uptake regulation in Caco-2 cells. Am J Physiol Cell Physiol 287:C1041–C1047.

Kipp H, Khoursandi S, Scharlau D, Kinne RK. 2003. More than apical: Distribution of SGLT1 in Caco-2 cells. Am J Physiol Cell Physiol 285: C737–C749.

Kumar A, Tyagi NK, Goyal P, Pandey D, Siess W, Kinne RK. 2007a. Sodium-independent low-affinity D-glucose transport by human sodium/D-glucose cotransporter 1: Critical role of tryptophan 561. Biochemistry 46:2758–2766.

Kumar A, Tyagi NK, Kinne RK. 2007b. Ligand-mediated conformational changes and positioning of tryptophans in reconstituted human sodium/D-glucose cotransporter1 (hSGLT1) probed by tryptophan fluorescence. Biophys Chem 127:69–77.

Lin JT, Kormanec J, Wehner F, Wielert-Badt S, Kinne RK. 1998. High-level expression of Na+/D-glucose cotransporter (SGLT1) in a stably transfected Chinese hamster ovary cell line. Biochim Biophys Acta 1373:309–320.

Miranda FF, Teigen K, Thorolfsson M, Svebak RM, Knappskog PM, Flatmark T, Martinez A. 2002. Phosphorylation and mutations of Ser(16) in human phenylalanine hydroxylase. Kinetic and structural effects. J Biol Chem 277: 40937–40943.

Miranda FF, Thorolfsson M, Teigen K, Sanchez-Ruiz JM, Martinez A. 2004. Structural and stability effects of phosphorylation: Localized structural changes in phenylalanine hydroxylase. Protein Sci 13:1219–1226.

Prince LS, Tousson A, Marchase RB. 1993. Cell surface labeling of CFTR in T84 cells. Am J Physiol 264:C491–C498.

Raja MM, Tyagi NK, Kinne RK. 2003. Phlorizin recognition in a C-terminal fragment of SGLT1 studied by tryptophan scanning and affinity labeling. J Biol Chem 278:49154–49163.

Tyagi NK, Goyal P, Kumar A, Pandey D, Siess W, Kinne RK. 2005. High-yield functional expression of human sodium/d-glucose cotransporter1 in Pichia pastoris and characterization of ligand-induced conformational changes as studied by tryptophan fluorescence. Biochemistry 44:15514–15524.

Vivian JT, Callis PR. 2001. Mechanisms of tryptophan fluorescence shifts in proteins. Biophys J 80:2093–2109.

Wright EM, Hager KM, Turk E. 1992. Sodium cotransport proteins. Curr Opin Cell Biol 4:696–702.

Wright EM, Loo DD, Turk E, Hirayama BA. 1996. Sodium cotransporters. Curr Opin Cell Biol 8:468–473.

Wright EM, Hirsch JR, Loo DD, Zampighi GA. 1997. Regulation of Na+/glucose cotransporters. J Exp Biol 200:287–293.